Late Occupation of the High-Elevation Northern Tibetan Plateau Based on Cosmogenic, Luminescence, and Radiocarbon Ages

P. Jeffrey Brantingham,[1,*] Gao Xing,[2] David B. Madsen,[3] David Rhode,[4] Charles Perreault,[5] Jerome van der Woerd,[6] and John W. Olsen[7]

[1]Department of Anthropology, University of California Los Angeles, Los Angeles, California
[2]Institute of Vertebrate Paleontology and Paleoanthropology, Chinese Academy of Sciences, Beijing, China
[3]Texas Archaeological Research Lab, University of Texas, Austin, Texas
[4]Desert Research Institute, Reno, NV
[5]Department of Anthropology, University of Missouri, Columbia, Missouri
[6]Institut de Physique du Globe de Strasbourg, CNRS Université de Strasbourg, Strasbourg cedex, France
[7]Department of Anthropology, University of Arizona, Tucson, Arizona

Correspondence
Corresponding author;
E-mail: branting@ucla.edu

Received
14 October 2010
Accepted
14 May 2013

Scientific editing by Steven L. Kuhn

Published online in Wiley Online Library (wileyonlinelibrary.com).

doi 10.1002/gea.21448

^{10}Be-^{26}Al cosmogenic surface exposure, optically stimulated luminescence, and radiocarbon dates from the site of Xidatan 2 (~4300 m above sea level [asl] in the Kunlun Pass, northern Tibetan Plateau) suggest the site was intermittently and briefly occupied approximately 9200–6400 yr B.P. This age is substantially younger than expected given the late Upper Paleolithic character of the lithic assemblage, which is dominated by microlithic and unique discoidal prepared core technologies. Comparisons between Xidatan 2 and known surface lithic assemblages in the Kekexili and Chang Tang regions of the central high Plateau show not only that the latter are technologically similar to Xidatan 2, but also that they are demonstrably connected to Xidatan 2 through utilization of the same stone raw materials, which includes a chemically distinctive obsidian. Contrary to most accounts of Tibetan Plateau colonization, our results suggest that the earliest substantial occupations on the interior Tibetan Plateau above 4000 m asl may date to the Pleistocene/Holocene transition.

INTRODUCTION

The Tibetan Plateau provides a unique opportunity to test fundamental models concerning the human capacity to colonize radically different and extreme environments. At the outset of our research program, we hypothesized that the northern Tibetan Plateau was colonized in several discrete stages coinciding with major fluctuations in regional paleoclimate, and that each discrete stage of colonization involved different forms of hunter-gatherer foraging organization (Brantingham et al., 2003). Our models have focused on the principal elevation steps of the northern Plateau: (1) the low-elevation areas surrounding the Plateau below 3000 m above sea level (asl), consisting primarily of Gansu Province, Ningxia, Inner Mongolia, and Xinjiang; (2) the middle-elevation step, between 3000 and 4000 m asl, including the large internal lake basins of Qinghai Province; and (3) the high-elevation step above 4000 m asl, including portions of Qinghai Province and the Tibetan Autonomous Region (Figure 1). Elsewhere, we have reported on archaeological fieldwork relevant to understanding the late Pleistocene occupation of the low-elevation areas surrounding the northern Tibetan Plateau both prior to and following the Last Glacial Maximum (LGM, ~25–15 ka; Madsen et al., 1998; Brantingham et al., 2000; Brantingham, Olsen, & Schaller, 2001; Madsen et al., 2001; Brantingham et al., 2004; Gao et al., 2004; Ji et al., 2005; Barton, Brantingham, & Ji, 2007). The evidence suggests that these low-elevation areas were colonized by early Upper Paleolithic foragers around 30 ka, a period characterized by the expansion of vast steppe grasslands through what is now desert northwest China. Recognized by the use of Levallois-like large-blade technologies, these early Upper Paleolithic populations engaged in high-frequency mobility strategies aimed at

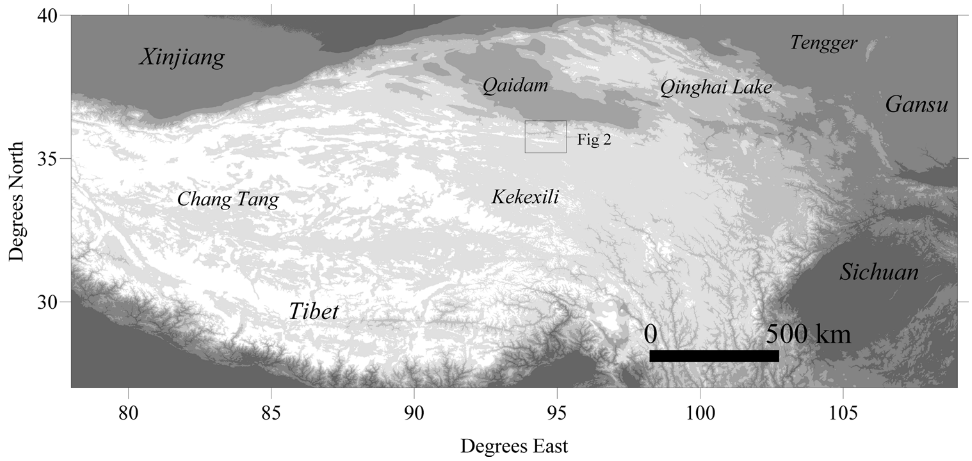

Figure 1 Digital elevation model showing the low- (Gansu, Xinjiang, < 3000 m asl), middle- (Qinghai Lake, Qaidam, 3000–4000 m asl), and high-elevation (Kekexili, Chang Tang, > 4000 m asl) steps of the Tibetan Plateau. Elevation increases with lighter shading. The location of Figure 2 is shown.

procuring high-ranked game and were probably organized in small, autonomous social groups. We proposed that these early Upper Paleolithic foragers may have occasionally moved onto the middle-elevation step of the Plateau as a by-product of their high mobility land use strategy (Brantingham et al., 2003). It was suggested, moreover, that the earliest exploitation of the high-elevation step of the Plateau may have occurred during the LGM when hyperaridity in the Qaidam basin may have pushed foragers up in search of more mesic conditions. Our work in the low-elevation environments surrounding the northern Tibetan Plateau indicates that following the LGM late Upper Paleolithic foragers shifted to the use of specialized microblade technologies and were probably engaged in more intensive exploitation of resources in patchy environments. We proposed that these late Upper Paleolithic foragers recolonized the middle- *and* high-elevation steps of the Plateau, but this time possibly as larger foraging parties targeting specific high-elevation resources (Brantingham et al., 2003).

Several features of this model of initial Plateau colonization have proven to be wrong. While evidence from the Qinghai and Qaidam basins broadly confirms the hypothesis that late Upper Paleolithic foragers engaged in seasonal exploitation of the middle-elevation step of the northern Plateau (Madsen et al., 2006; Rhode et al., 2007), there is scant evidence for human occupation of the Tibetan Plateau before 15,000 yr B.P. (Brantingham & Gao, 2006; Brantingham, Gao, Olsen, et al., 2007). We have shown that climatic and environmental conditions on the middle-elevation step of the Tibetan Plateau during marine isotope stage (MIS) 3 (45–25 ka) were significantly more extreme than previously envisioned (Madsen et al., 2008; Rhode et al., 2009), providing little incentive for early Upper Paleolithic foragers in northwest China to move into higher elevations.

The timing of the earliest occupation of the high-elevation step of the Plateau above 4000 m asl is also seriously in question. None of the more than 20 stone tool-dominated surface assemblages known from the high-elevation step of the Tibetan Plateau has been directly dated (but see Zhang & Li, 2002; Aldenderfer, 2007; Yuan, Huang, & Zhang, 2007). As a consequence, researchers have tended to rely on coarse-grained techno-typological comparisons with lithic assemblages from in lower elevation environments to infer ages of colonization. For example, the presence of simple retouched side scrapers and discoid-like flake cores, which are broadly similar to Middle Paleolithic technologies seen in North China, has been used to argue for a pre-LGM occupation of the high Plateau (An, 1982; Huang, 1994; Brantingham, Olsen, & Schaller, 2001; Aldenderfer, 2003; Aldenderfer & Zhang, 2004). Brantingham et al. (2001) argued that the specialized large blade and bladelet technologies seen in the Chang Tang region of northern Tibet were derived from, and therefore are younger than, the early Upper Paleolithic seen in Northwest China at around 30 ka. They suggested that these technologies possibly represented an LGM (*ca.* 25–15 ka) occupation of the high Plateau. Microblade technologies found in abundance in surface contexts across the northern Plateau are characteristic of the late Upper Paleolithic in Northwest China (*ca.* 15–11 ka), suggesting that they appeared on the high Plateau sometime shortly after the LGM. In sum, the lithic techno-typological evidence has been used to suggest that the high-elevation step of the Tibetan Plateau was repeatedly colonized before, during, and after the LGM. Here we show that this hypothesis may be wrong and that the oldest substantial occupation of the high-step of the Tibetan Plateau dates to well after the LGM.

We report on initial archaeological research at the Xidatan 2 site (*ca.* 4300 m asl) in the Kunlun Pass area, Qinghai Province, China, the primary high mountain pass between the middle- and high-elevation steps of the northern Tibetan Plateau. ^{10}Be cosmogenic surface exposure ages (Van Der Woerd et al., 2002), combined with optically stimulated luminescence (OSL; Owen et al., 2006) and radiocarbon dates, indicate Xidatan 2 was occupied sometime between approximately 9200–6400 yr B.P., with a concentration of human activity at the site perhaps around 8000–7000 yr B.P. These ages are much younger than expected given the prominence of bipolar and both microlithic and discoidal prepared core technologies in the assemblages. In combination, these technologies are more characteristic of the late Upper Paleolithic than of the epi-Paleolithic, as suggested by the chronology. The types of stone raw materials present at Xidatan 2 are unusually diverse and include a chemically unique obsidian. This obsidian is found at other sites on the high Plateau and has been discovered at an early Holocene site on the southern shore of Qinghai Lake, nearly 1000 km from the source (Rhode et al., 2007). The transfer of obsidian toolstone to the Qinghai Lake basin also suggests that regular movement of groups between the high- and middle-elevation steps was established by at least 9200–6400 yr B.P. These data demonstrate that utilization of the Kunlun Pass-Xidatan area was connected with regular exploitation the high Plateau to the south and implies also that the known surface lithic assemblages in the Chang Tang and Kekexili areas of the northern Plateau date to the Pleistocene/Holocene transition, much later than previously thought (Brantingham, Olsen, & Schaller, 2001; Brantingham et al., 2003). These widely dispersed sites may have been part of a single postglacial settlement system on the high Plateau. This conclusion is further supported by the striking similarity between the lithic technologies seen at Xidatan 2, and the Kekexili and Chang Tang surface localities. A similar assemblage composed of bladelet and microblade technology from the Xiadawu site (4000 m asl), in the Maqu (Yellow River) segment of the Kunlun range, is radiocarbon dated as early as 11,900 cal. yr B.P. (Van Der Woerd et al., 2002). It remains uncertain, however, in all of these cases, whether exploitation of the high Plateau during the early Holocene was year-round or seasonal. We discuss these findings in light of the regional archaeological and paleoclimatic sequence.

Geographic Setting

The northern Tibetan Plateau is divided into two elevational steps by tectonic structures associated with the Himalayan-Tibetan orogeny (Figure 1; Yin & Harrison, 2000; Tapponnier et al., 2001). The middle-elevation step, between approximately 3000 and 4000 m asl, is bounded by the Altyn Tagh–Qilian mountain ranges in the north and the Muzutag–Kunlun–Anyimaqen ranges in the South. These ranges reach maximum elevations of 5500 m and 7500 m asl, respectively. The middle-elevation step of the Plateau is dominated by two major internal drainage basins, the Qinghai Lake basin in the East and greater Qaidam basin in the West. We discuss the geology and archaeology of the Qinghai Lake basin elsewhere (Madsen et al., 2006; Rhode et al., 2007; Madsen et al., 2008). The greater Qaidam basin is a syncline located between approximately N36–39° and E91–98° (Tapponnier & Molnar, 1977; Tapponnier et al., 2001).

Climate and environment in the Qaidam is influenced by the rain shadow of the high-elevation step of the Plateau, by the westerly jet stream, and by the Siberian high-pressure cell, also referred to as the East Asian Winter Monsoon (Benn & Owen, 1998; Owen et al., 2006). Mean annual precipitation across the greater Qaidam ranges from <25 to 50 mm and mean annual temperatures are between 2 and 4°C (Yang et al., 2004). Permafrost is limited to the higher elevations in the surrounding mountain ranges, although the entire middle-elevation step of the Plateau experiences seasonally frozen ground (Wu et al., 2005). Vegetation trends from steppe-grassland to desert-steppe and Gobi as one moves from east to west across the basin (Lehmkuhl & Haselein, 2000).

The high-elevation step of the Tibetan Plateau (Figure 1) is bounded on the north by the Muzutag–Kunlun–Anyimaqen mountain ranges. The Greater Himalaya form a southern boundary, approximately 1000 km to the south. The high Plateau has an average elevation of more than 5000 m asl with very little topographic relief in the interior (Fielding et al., 1994; Yin & Harrison, 2000). The topographic boundaries of the high Plateau, by contrast, are characterized by changes in elevation of as much as 2000–3000 m over distances of only 100–200 km (Fielding et al., 1994). The limited topographic relief of the interior of the high Plateau means that there is little active erosion, alluvial drainages are relatively short, and small, shallow lakes are common (Jin et al., 2005). Precipitation on the high Plateau derives primarily from the South Asian Summer Monsoon and mean annual precipitation for the entire high Plateau (*ca.* 318 mm/year) exceeds that seen on the middle-elevation step (Schaller, 1998: 29; Morrill, Overpeck, & Cole, 2003). However, the influence of the South Asian Summer Monsoon decreases from southeast to northwest such that conditions on the northern portions of the high Plateau are substantially more arid than on the southern portion. Precipitation along the Muzutag–Kunlun–Anyimaqen boundary is predominantly orographic, though there may also be some contribution from the westerly jet stream (Benn & Owen, 1998; Owen et al., 2006). Mean annual temperatures are low (*ca.* −2 to −4°C for the high Plateau overall) and extensive soil permafrost is supported in most areas above 4400 m (Wu et al., 2005). Environments of the high Plateau reflect these climatic conditions. The environment outside of the Indus, Sutlej, and Tsangpo River drainages in the south is characterized as alpine desert-steppe (Schaller, 1998).

The Kunlun Pass is a key mountain pass between the middle and high-elevation steps of the Plateau in the eastern Kunlun range (Li, Yin, & Yu, 2000; Wu et al., 2001). It would have likely served as one of the major corridors for human population movements onto the high Plateau. The Kunlun Pass thus might be expected to provide evidence for the timing and nature of such movements. The pass is divided into three sections (Figure 2). The Kunlun Pass proper is a small depositional basin formed around a short thrust fault—the Kunlun Pass fault—associated with the 1600 km long primary Kunlun strike-slip fault (Wu et al., 2001; Van Der Woerd et al., 2002). The pass lies at an elevation of 4600 m asl with hills on either side of the pass rising to approximately 4800 m. The Kunlun Pass Fault creates a gap through the Burhan Budai Shan (maximum elevations approximately 6210 m asl) and lies to the south of the Xidatan-Dongdatan-Maqu valley, a pull apart trough along the main segment of the Kunlun Fault (Van Der Woerd et al., 2002). The Xidatan-Dongdatan-Maqu valley lies between 4300 and 3700 m asl and connects, via the Xiaonanchuan drainage, with the Yeniugou-Golmud River valleys (Wu et al., 2001). The distal section of the valley corridor enters the Qaidam basin at an elevation of around 3000 m asl near the modern city of Golmud (Li, Yin, & Yu, 2000). The total elevation difference along the Kunlun Pass and valley corridor is approximately 2000 m over a distance of only 120 km. Climatic and environmental conditions are radically different at the two endpoints of the corridor. Mean annual temperatures decline from approximately 1 to 2°C at Golmud to between −2 and −3.5°C at Xidatan. Mean annual temperatures reach −6 to −5°C at Wudaoliang, approximately 110 km south of the Kunlun Pass at an elevation of 4800 m asl. Mean annual precipitation increases from 31.6 mm at Golmud to 287 mm at Xidatan and 264 mm at Wudaoliang (Harris, Cui, & Cheng, 1998). Environments change accordingly from unvegetated bajadas and Gobi-type surfaces at the entrance to the Qaidam basin to alpine desert-steppe where the Kunlun Pass emerges onto the high Plateau.

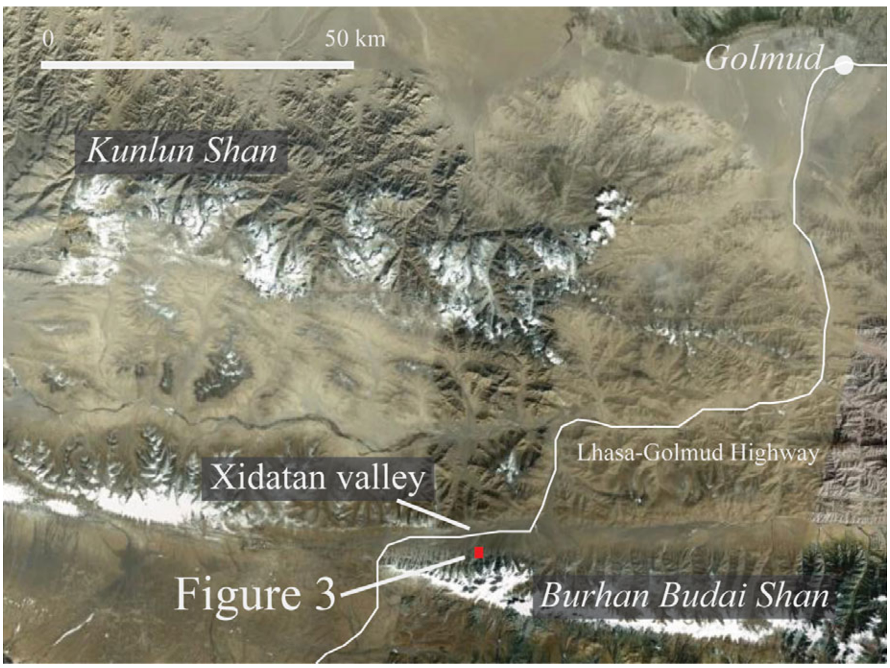

Figure 2 Google Earth image of the Kunlun Pass area showing the location of Xidatan 2 detailed in Figure 3. Golmud lies at an elevation of approximately 3000 m above sea level (asl). The Burhan Budai shan reaches peak elevation of 6210 m asl Xidatan 2 is at 4300 m asl.

RESULTS

Xidatan 2 Geomorphology and Stratigraphy

The Kunlun River flows west through the Xidatan portion of the Xidatan-Dongdatan-Maqu valley at approximately 4000 m asl. It makes an abrupt turn north through the Xiaonanchuan drainage, at approximately N35.75° and E94.33°, where it joins the Golmud River. The local glacial equilibrium line elevation is approximately 5200 m asl allowing the Burhan Budai Shan to support modern valley glaciers that extend north through steep glacial-cut valleys to terminate at approximately 4560 m asl (Van Der Woerd et al., 2004; Owen et al., 2006). The current minimum elevation of permafrost in the Xidatan area is 4385 m, 25 m above its known location in 1975 (Wu et al., 2005). However, seasonally frozen ground is characteristic of the entire area. Lateral moraines representing at least two periods of glacial advance from the Burhan Budai Shan are in evidence in valleys along the Xidatan segment at elevations of 4418–4546 m asl (M2) and 4803–4945 m (M1) in the valley studied by Owen et al. (2006: Table II). Glacially fed stream terraces with steep cut risers line the modern drainages below the moraines (Van Der Woerd et al., 2002). These terraces coalesce into alluvial bajadas that fill the valley floor where the glacially fed streams meet the Kunlun River. Field studies and surface exposure dating (see below) conducted by van der Woerd et al. (2002) show that the terraces in the Xidatan-Dongdatan segment fall into five distinct age sets (T1–T5). Individual drainages appear to contain at most three of these, either T1–T2–T3 or T3–T4–T5, in addition to the modern active stream bed (T0; Van Der Woerd et al., 2002).

Similar fluvial terraces are found slightly downstream in the Kunlun/Golmud River system. Chen et al. (2011) defined four strath terraces in the Xiaonanchuan segment 4–14 km from the nearest Burhan Budai Shan terraces, while Wang et al. (2009) identified five terraces in the Nachitai segment immediately downstream from the Xiaonanchuan segment. However, the fluvial terraces in the Kunlun/Golmud River drainages are discontinuous and it is difficult to extrapolate the terraces sequence from one river segment to another with any degree of confidence. Chen et al. (2011; see also Wang et al., 2009) suggest deposition of the alluvial fill of the Kunlun/Golmud River valley and the development of the alluvial fans along its margin occurred about 82–16 ka during a period they term the Sanchahe depositional stage. This depositional stage was followed by a postglacial period of tectonic uplift that led to river entrenchment and development of the fluvial terrace sequences. Similarly, van der Woerd et al. (2002) suggest the oldest T5 terrace at Xidatan 2 "corresponds to the ancient fan surface" prior to incision. Here, we provide a recalculated average ^{10}Be-^{26}Al cosmogenic age of 15,777 ± 669 yr B.P. for cobbles on the T5 surface at Xidatan 2 (see below). This age suggests the ancient alluvial fans into which the glacially fed Burhan Budai Shan streams are inset are equivalent to the Sanchahe depositional stage.

Loess overlies the outwash debris on all terraces above the modern drainages and is correlated with loess layers in similar stratigraphic positions in the adjacent Yeniugou segment of the Kunlun/Golmud River drainage (Owen et al., 2006) and in the Xiaogangou segment (Chen et al., 2011). The loess cap in the Xidatan area varies in thickness from <0.3 m, on the lower terraces, to approximately 2 m on the higher terraces, and is stabilized by dense cushion plant cover. The loess thickens upslope near the mountain front where rising wind currents lose their capacity to carry sediment. On the higher terraces the loess is eroded in places through a combination of burrowing by black-lipped pika (*Ochotona curzoniae*; Schaller, 1998) and possibly seasonal freeze-thaw cycles (Wu et al., 2005). Both processes lead to the separation of loess particles from the dense root mass that serves to otherwise stabilize the sediments. Strong local winds mobilize the resulting loose sediments leaving irregularly patterned blowouts between intact loess stacks.

Xidatan 2[1] is an archaeological locality consisting of stone tool reduction debris found on the fourth terrace (T4) of an unnamed drainage at approximately N35.71° and E94.26° (Figure 3). T4 is divided into southern and northern sections by the Kunlun Fault. Here the fault is characterized by a lateral slip offset of approximately 110 m and short pressure ridges approximately 20 m high (Van Der Woerd et al., 2002). The southern section of T4 is approximately 386 m in length, 100 m wide, and dips north at about 8°. The northern section merges gradually with the valley bajada. Archaeological materials are found along the entire length and width of the southern T4 section, but with concentrations of lithic artifacts centered on the middle portion of the terrace (Figure 4). Only a handful of artifacts were found on the northernmost T4 section. Surface survey failed to identify artifacts on either T3 or T5.

Most of the lithic specimens on T4 were found at the surface in blowouts between intact loess stacks. We conducted a small test excavation centered on a dense concentration of surface artifacts and incorporating an intact loess stack to determine if subsurface archaeological

[1]This archaeological locality is in the same location as Van der Woerd et al.'s (2002) Site 2. We have adopted their numbering to aid in comparison across these research projects.

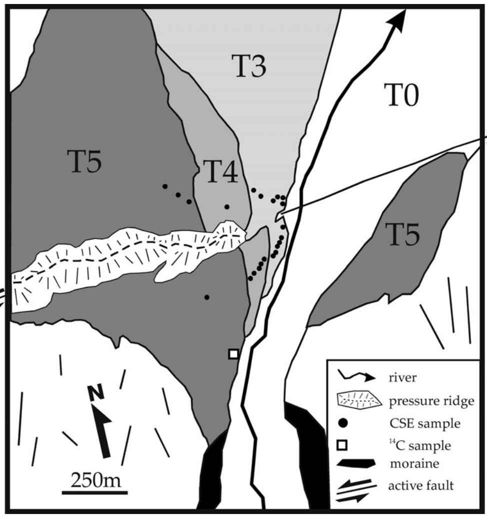

Figure 3 Plan view of the three glacial outwash terraces at Xidatan 2. All three terraces are preserved on the western side of the drainage, but only T5 is preserved on the eastern side. The western terraces are offset by an active segment of the Kunlun fault that has generated an approximately 10 m high pressure ridge. The Xidatan 2 archaeological site is located on the section of T4 south of the Kunlun fault. Redrawn after Van der Woerd et al. (2002).

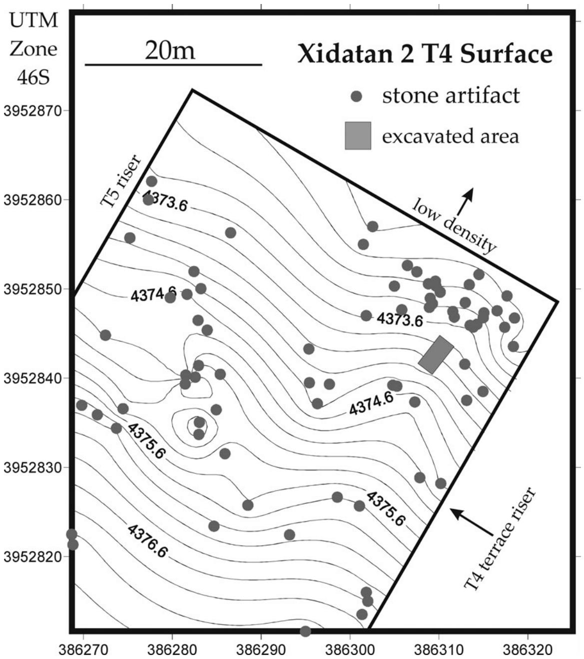

Figure 4 Distribution of lithic finds on the T4 surface at Xidatan 2. Map axes are given in UTM coordinates and elevation contours are meters asl.

materials were present in the loess and to assess the nature of the relationship between surface and any subsurface materials. A 4 × 2 m unit was excavated down to a contact with the angular gravels that compose the T4 glacial outwash fill. Sediments within the intact loess block are divided into three horizons: (1) a dense upper rootlet zone with abundant dark organic matter (5–8 cm thick); (2) a moderately dense root zone with minor organic content and unweathered loess (12–20 cm thick); and (3) unweathered loess with only rare rootlets (10–12 cm thick). A total of 31 lithic artifacts were recovered from subsurface contexts, representing 18% of the total collection. Artifacts are present throughout Horizons 2 and 3 down to a depth of approximately 8–10 cm above the terrace gravels. The majority of the *in situ* artifacts, including two large quartzite flakes, were found lying flat along the contact between the Horizons 2 and 3 at a depth of 15–30 cm below surface. This, and the presence of small pea-sized gravel concentrated at the same depth, suggests that the Horizon 2/3 contact may represent a temporarily stable land surface occupied by foraging groups. The presence of materials on the surface as well as throughout most of the upper Horizon 2 suggests the site may have been intermittently occupied several times.

A 5-cm-thick by 40-cm-long concentration of charcoal was exposed in the upper loess of the T5 terrace, 16 cm below the surface and 125 cm above the T5 gravels, approximately 100 m upstream from the center of the main lithic concentration on T4 (Figure 3). While no lithic materials were directly related to the charcoal lens, its concentrated nature, morphology, and the lack of charcoal elsewhere in the more than 200 m of exposed loess, suggests it may have been an isolated hearth rather than the result of a natural fire. Given the absence of archaeological materials on T5, we assume that this feature is related to the T4 materials and use the obtained AMS ^{14}C date to help constrain the age of the Xidatan 2 occupation (see below).

Xidatan 2 Lithic Assemblage

The Xidatan 2 lithic assemblage is diverse both in terms of raw material types and technologies represented. The assemblage is broadly characteristic of the northeast Asian late Upper Paleolithic containing both casual flake tools and specialized microblade cores and microblades (Elston et al., 1997; Lie, 1999; Zhang, 1999; Elston & Brantingham, 2002). A total of 172 specimens were recovered from both surface and stratified contexts at the site. Seven broad classes of raw material are present in the assemblage, most notably artifacts made on a chemically distinctive true obsidian glass (Table I). Based on color differences, there may be as many as 20 unique raw material varieties including five varieties of quartzite and seven varieties of cryptocrystalline silicates (i.e., chert).

Table I Stone raw material types from Xidatan 2.

	Raw Material Type (*n* specimens)								
Munsell Color Description	Quartzite	CCS[a]	Jasper	Mudstone	Obsidian	Vein Quartz	Quarz Crystal	Metamorphic	Total
Translucent		1			3[b]				1
Black to dark gray	34	30							64
Gray		1		1					2
Very dark to light greenish-gray	43	3	5					2	53
Dark gray to light gray and light olive gray	21	1							22
White	5	1				5	1		12
Light yellowish-brown to grayish-brown	5			4[c]					5
Dark brown and grayish-brown		1							1
Dusky red									5
Total specimens	108	38	5	5	3	5	1	2	172
Number of raw material varieties	5	7	2	2	1	1	1	1	20

[a]Crypto-crystalline silicate.
[b]Source is 416 km southwest of Xidatan 2 at Migriggyangzham Co.
[c]Source is 66 km south of Xidatan 2 at the Police Station 1 site.

Raw material source locations are known for only two of the raw materials represented. A light yellowish-brown to grayish-brown mudstone originates from deposits around several active springs at the Police Station 1 and 2 sites (N35.43°, E93.61°, 4451 m asl), approximately 66 km south of Xidatan 2 (Brantingham & Gao, 2006; Brantingha, Gao, Olsen et al., 2007). Obsidian artifacts chemically identical to that from Xidatan 2 have been identified at four other archaeological sites on the Plateau (Figure 5). Most of these sites are on the high Plateau south of Xidatan 2, but one (Jiangxigou 2) is on the southern shore of Qinghai Lake (Brantingham & Gao, 2006; Brantingham, Gao, Olsen et al., 2007). The geological source of this material is reported to be centered around Migriggyangzham Co (N33.42°, E90.30°, 5240 m asl; the Shuanghu site of Brantingham, Olsen, & Schaller [2001]). Well-rounded, cobble to large pebble-sized obsidian nodules are found in surface contexts around Migriggyangzham Co and represent either volcanic bombs, or remaining lag from an eroded fused tuff. Xidatan 2 is approximately 416 km from the reported obsidian source, while the other known archaeological examples of this material on the high Plateau are 171 km (Dogaicoring), 243 km (Erdaogou), and 350 km (Police Station 1) from the source. The Jiangxigou 2 site, which has yielded several examples of this material and is radiocarbon dated between 9140 ± 90 and 5580 ± 60 cal. yr B.P. (Rhode et al., 2007), is on the southern shore of Qinghai Lake, 551 km from Xidatan 2 and 951 km from the source.

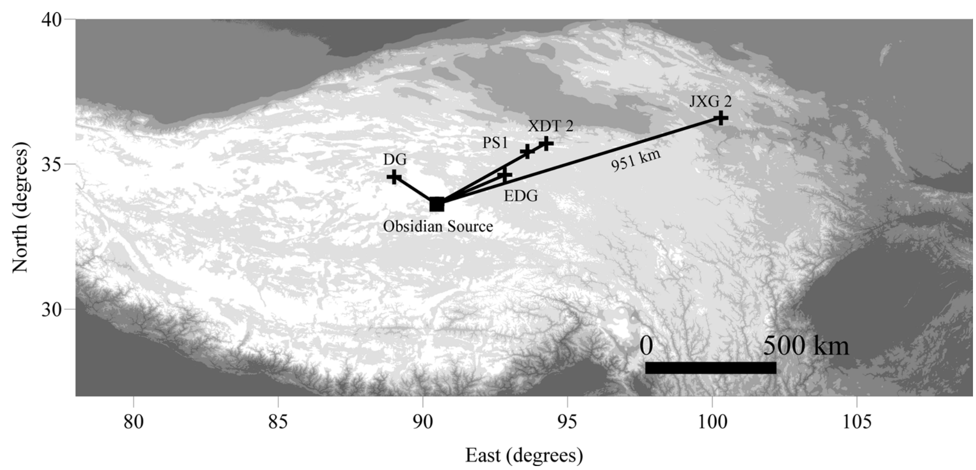

Figure 5 The distribution of known archaeological sites containing Plateau obsidian and the location of the source. DG, Dogaicoring; EDG, Erdaogou; PS1, Police Station 1; XDT 2, Xidatan 2; JXG 2, Jiangxigou 2.

Table II General technological types from Xidatan 2.

	Raw Material Type							
	Quartzite	CCS[a]	Jasper	Mudstone	Obsidian	Vein Quartz	Metamorphic	Total
Flaked piece (core)	5		1	1		1		8
Detached piece (flake)	79	26	5	3	1	1	3	118
Retouched tool	4				2			6
Core and flake shatter	20	13	3	1		3		40
Total	108	39	9	5	3	5	3	172

[a]Crypto-crystalline silicate.

The Xidatan 2 lithic assemblage includes pieces representative of stone core reduction, but very few specimens recognized as formal retouched tools (Table II). Cores fall into three broad technological categories including generalized flake cores (Figure 6). A bifacial discoid reduction strategy is also seen here. Despite the classification, this core technology is only superficially similar to the bifacial discoids seen at Middle Paleolithic sites in North China, such as Zhoukoudian Locality 15 (Gao, 2000). In the case of Xidatan 2, following centripetal preparation of both core faces, a series of circular, tablet-like flakes with trapezoidal cross sections were detached parallel to the plane of intersection between the faces (Figure 6e, f). One specimen, casually retouched along one edge, indicates that these circular flakes were worked into tools. This technology, though very unusual in flaking procedure, shares much in common with techniques for microblade core platform rejuvenation, and we suspect that it is in fact derived from Northeast Asian microblade technologies, though it is applied to a large flake-core substrate.

The other prominent core technology at Xidatan 2 is represented by classic northeast Asian microblade cores (Elston & Brantingham, 2002). Typically, small pebbles or thick flakes of high quality stone materials were shaped into wedge-shaped, bullet-shaped, or cylindrical core forms. Small (~30–50 mm long, 5–8 mm wide) blades were produced sequentially from the reduction face, which is positioned approximately perpendicular to the striking platform. At Xidatan 2, two complete

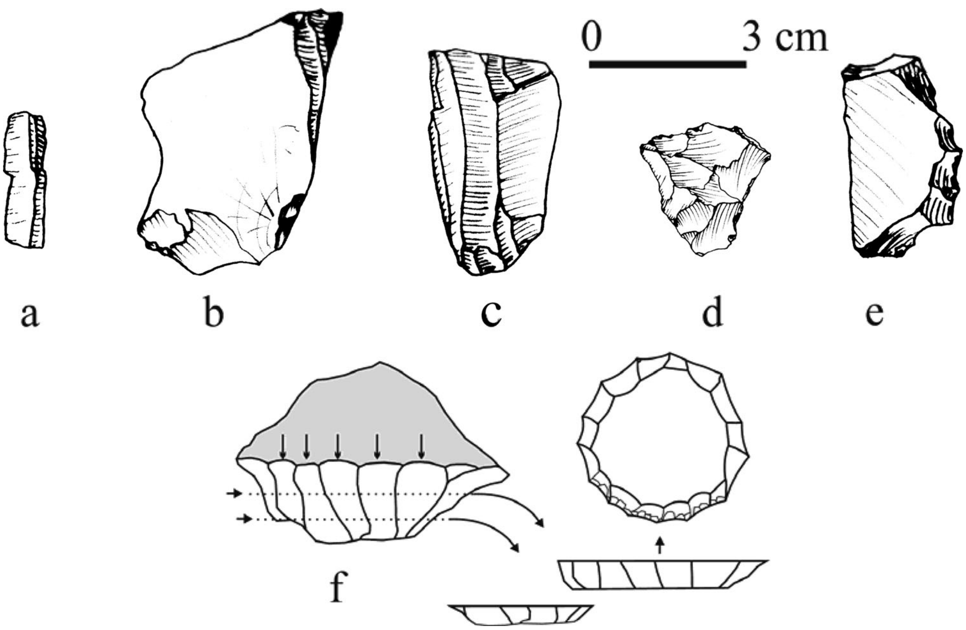

Figure 6 Lithic specimens from Xidatan 2. (a) Microblade; (b) microblade core perform on fined-grained gray quartzite; (c) microblade core on cream-colored mudstone from the Police Station 1 spring deposits; (d) heavily retouched flake made on Chang Tang obsidian; (e) flat, tablet-like flake removed from the face prepared discoidal core made on gray-green quartzite; (f) the proposed reduction sequence for the discoidal prepared cores seen at Xidatan 2 involves standard reduction of a bifacial discoid followed by removal of one or more tablet like flakes and subsequent retouching of these flakes into circular flake tools.

Table III Xidatan 2 core, flake and tool types.

	Raw Material Type (*n* specimens)							
	Quartzite	CCS	Jasper	Mudstone	Obsidian	Vein Quartz	Metamorphic	Total
Core types								
Discoidal	1							1
Microblade	1	1		1				3
Tested pebble	2					1		3
Total	4	1		1		1		7
Flake types								
General flake	69	16	5	2	1	1	3	97
Bipolar flake	3							3
Flake-blade	3			1				4
Microblade	1	10						11
Discoid edge element[a]	4							4
Total	80	26	5	3	1	1	3	119
Tool types								
Scraper	2[b]							2
Retouched flake	1							1
Combination tool					1[c]			1
Retouched point					1			1
Total	3				2			5

[a]Flake removing all or part of the edge of a core.
[b]Both specimens are burin-like resharpening spalls with remnant scraper retouch.
[c]Combines a scraper edge and retouched notch.

microblade cores, one made on Police Station 1 mudstone and another on green jasper, and one unfinished core on fine-grained black to dark gray quartzite, were recovered (Figure 6b, c). Two of the cores are based on flake blanks, while the original blank type for the third core is obscured because it is heavily reduced into a "bullet" form.

Flakes with intact platforms comprise the bulk of the assemblage (Table III). Flakes based on quartzite dominate followed by those on cryptocrystalline materials. Generalized flakes and microblades are the two most common flake types. These, along with discoid edge elements, which are analogous to the technical pieces typically removed from Levallois core edges (Kuhn, 1995), are consistent with the technologies represented in the core sample. However, bipolar technology makes up a small, but distinctive (see Madsen et al., 2001; Barton, Brantingham, & Ji, 2007) component of both the flake assemblage and flake shatter.

Six lithic specimens preserve evidence of formal retouch, comprising only 3% of the total assemblage. Three are complete retouched tools of fairly generic design and two of these are based on Plateau obsidian (Figure 6d). One specimen is a casually retouched circular flake detached from the upper surface of a discoid prepared core (Figure 6e). The two remaining specimens should be classified technically as debitage; these are burin-like spalls that preserve scraper-like retouch along one side and are most likely by-products of tool resharpening. Many of the 27 microdebitage specimens, all weighing less than 1 g, are also consistent with tool resharpening activities. Brantingham, Olsen, and Schaller (2001) observed that the cores, flakes, and tools from the Chang Tang on the high Plateau displayed heavy resharpening and recycling and Xidatan 2 appears to be similar in this respect.

Geochronology at Xidatan 2

The age of the Xidatan 2 assemblage is constrained by a combination of cosmogenic surface exposure and AMS ^{14}C dates. OSL dates on loess from contexts in the Kunlun/Golmud River drainage system also provide important local geochronological information. OSL and cosmogenic dates are in calendar years before present, which is defined as the year of publication of the results. Cosmogenic surface exposure ^{10}Be-^{26}Al ages for each of the three glacial outwash terraces at Xidatan 2 were determined as part of a study of slip rates along a segment of the Kunlun fault, which runs approximately E-W through the site (Ryerson et al., 1998; Van Der Woerd et al., 2002). Cosmogenic surface exposure dating is based on *in situ* production of radioactive or stable nuclides (isotopes) in rock minerals of certain types (Lal, 1991; Gosse & Phillips, 2001; Stone, 2000; Faure & Mensing, 2005). The time since a rock or clast was initially exposed is determined from the concentration of cosmogenic nuclides given known production rates, while taking into account the effects of erosion and radioactive decay. At Xidatan 2, van der Woerd et al. (2002) selected and dated clasts exposed on the surface of each of the terraces (see Figure 3). Since the publication of that paper, however, cosmogenic nuclide production curves have been revised (e.g., Nishiizumi et al., 2007) and we have recalculated the Xidatan 2 ^{10}Be-^{26}Al ages using the CRONUS-Earth on-line calculator (Balco et al., 2008) and a constant production rate model (Lal, 1991; Stone, 2000) with the assumption of negligible erosion (Table IV). Cosmogenic surface exposure ages typically show propagated errors on the order of $\pm$ 10% of the mean age. This is the case at Xidatan 2. For example, individual clasts from T5, T4, and T3 show ^{10}Be dates of 15,960 $\pm$ 1513 yr B.P. (KL17D-4), 9411 $\pm$ 1014 yr B.P. (KL16D-6), and 7219 $\pm$ 701 yr B.P. (KL15D-10), respectively. Following Van der Woerd et al (2002), we average the ^{10}Be and ^{26}Al ages for each sample if the ratio ^{26}Al age/^{10}Be age $\geq$ 0.7, favoring the ^{10}Be age otherwise. We then exclude outliers and calculate the weighted average ages across all remaining samples from T5, T4, and T3. The two stage averaging process has the effect of reducing the error bounds so that typical errors are around 4% of the mean. The weighted average ages for the T5, T4, and T3 surfaces are 15,777 $\pm$ 669 yr B.P. ($n = 3$), 9239 $\pm$ 361 yr B.P. ($n = 4$), and 7101 $\pm$ 165 yr B.P. ($n = 11$), respectively (Figure 7).

The results of ^{10}Be-^{26}Al surface exposure dating imply a relatively simple formation and exposure history for the Xidatan 2 outwash terraces (see Van Der Woerd et al., 2002; Figure 8). Fan incision began shortly after approximately 15.7 ka. This is the point at which the T5 surface became stabilized and at which the clasts began their exposure. The period of incision creating the T5 terrace riser is expected to have been short relative to the period in which the outwash debris accumulated to form the inset terrace T4. Aggradation of T4 terminated around 9.2 ka, when another period of incision began. T3 was abandoned at approximately 7.1 ka. While younger terraces are represented in other drainages in the Xidatan-Dongdatan valley (Van Der Woerd et al., 2002) and downstream along the Kunlun/Golmud River (Chen et al., 2011), these are not seen at Xidatan 2. Active flow in the modern drainage T0 appears to have eroded these younger features at Xidatan 2.

Similar fluvial terraces are found downstream from Xidatan 2 along the Sanchahe, Nachitai, and Xiaogangou segments of the Kunlun/Golmud River (Wang et al., 2009; Chen et al., 2011). Using a combination of OSL and radiocarbon dating techniques directly on terrace sediments and incorporating similar data from Wang, Wang, and Xiang (2003) and Wang et al. (2009), Chen et al. (2011) date the four terraces immediately below the surface of the MIS 3/2 alluvial fans to approximately 16 ka (T4), 13 ka (T3), 11 ka (T2) and 5 ka (T1). Since these features are discontinuous with the Xidatan terraces, however, it is difficult to determine if they resulted from the same tectonic events that led to the incision of the Xidatan terraces. As recognized by Van Der Woerd et al. (2002), not every drainage contains a complete sequence of terraces. If they are synchronous, then T5 at Xidatan 2 may correspond to T4 reported by Chen et al. (2011). T4 at Xidatan 2 may correspond to T2 reported by Chen et al. (2011), which is slightly older than the ^{10}Be surface exposure ages that Xidatan 2 indicate. We note that ^{10}Be-^{26}Al cosmogenic dating standards continue to evolve and some refinements to the Xidatan 2 age estimates may be necessary. Regardless of these possible refinements, it is clear that the initial occupation of Xidatan 2 dates to well after the LGM. We therefore use approximately 9200 yr B.P. as the limiting maximum age for the initial occupation of the Xidatan 2 archaeological site.

OSL and radiocarbon dates constrain the timing of loess deposition in the region, which is present as a sediment cap on both T4 and T5. Chen et al. (2011) obtained an OSL age of 13.9 $\pm$ 1.4 ka for a sample from the base of loess deposits overlying terrace gravels in Xiaogangou segment of the Kunlun/Golmud River 60 km downstream from the Xidatan segment at an elevation of approximately 3200 m asl (Figure 2). Owen et al. (2006) provide an OSL age of 8.6 $\pm$ 0.7 ka for a sample from swamp/lacustrine silts overlying alluvial fan deposits and immediately underlying an approximately 2 m thick loess cap at a location 36 km downstream in the Yeniugou-Golmud segment of the drainage (Figure 2). The two OSL dates are generally in accord with the ages of post-LGM loess deposition estimated at a number of other localities along the northeastern margin of the Tibetan Plateau that range from about 14 to 9 ka (e.g., Küster et al., 2006; Sun et al., 2007; Lu et al., 2011). The variation in these age estimates for the post-LGM loess deposition is due to local factors, such as the proximity to dust source areas, the nature of underlying sediments, microclimatic variation, and the timing of establishment of sufficient vegetation to capture and hold dust. Direct OSL dates on the Xidatan loess will be necessary to confirm the age of initial loess deposition on the Xidatan terraces. Here, we assume that the maximum age of the loess on T5 at Xidatan 13.9 $\pm$ 1.4 ka as determined by Chen et al. (2011) at the Xiaogangou section.

The minimum age of the occupation on T4 at Xidatan is constrained by an AMS ^{14}C date from the loess cap on the T5 terrace. Charcoal from a possible hearth, found at a depth of 16 cm below the modern ground surface and 125 cm above the outwash gravels on T5, yielded an age of 5630 $\pm$ 40 ^{14}C yr B.P. (Beta 194553) and a calendar age of 6404 $\pm$ 50 cal. yr B.P. (Intcal 09). Assuming an onset of

Table IV Analytical results of ^{10}Be and ^{26}Al cosmogenic isotope dating at Xidatan 2.[a]

Sample Name	Latitude (°N)	Longitude (°E)	Elevation (m asl)	Elevation Flag[b]	Sample Thickness (cm)	Density (g/cm^3)	Shielding Correction	Erosion Rate (mm/yr)	^{10}Be Conc. (at/g/yr)	Err ^{10}Be (at/g/yr)	AMS Standard	^{26}Al Conc. (at/g/yr)	Err ^{26}Al (at/g/yr)	AMS Standard	^{10}Be Model Age (yr B.P.)[c]	Err ^{10}Be (yr)	^{26}Al Model Age (yr B.P.)[c]	Err ^{26}Al (yr)
Terrace T3																		
KL15D-1X	36	94	4340	std	2	2.65	1	0	604,000	30,600	LLNL3000	3,060,000	153,000	KNSTD	7694	775	6677	671
KL15D-2	36	94	4340	std	2	2.65	1	0	526,272	21,355	KNSTD	1,653,680	63,835	KNSTD	7011	673	3603	343
KL15D-3	36	94	4340	std	2	2.65	1	0	0	0	KNSTD	2,920,737	104,312	KNSTD	–	–	6373	600
KL15D-4	36	94	4340	std	2	2.65	1	0	526,398	17,094	LLNL10000	2,959,441	127,976	KNSTD	7013	651	6457	629
KL15D-7	36	94	4340	std	2	2.65	1	0	591,218	41,192	KNSTD	1,510,000	186,983	KNSTD	7878	879	3290	498
KL15D-10	36	94	4340	std	2	2.65	1	0	541,863	23,361	KNSTD	3,078,552	127,143	KNSTD	7219	701	6718	648
KL15U-1	36	94	4340	std	2	2.65	1	0	560,000	24,575	KNSTD	3,620,000	117,000	KNSTD	7461	727	7904	735
KL15U-3	36	94	4340	std	2	2.65	1	0	560,589	33,723	KNSTD	3,460,000	220,000	KNSTD	7469	791	7554	816
KL15U-4	36	94	4340	std	2	2.65	1	0	564,618	23,420	KNSTD	3,040,000	118,000	KNSTD	7523	725	6634	633
KL15U-5	36	94	4340	std	2	2.65	1	0	1,080,000	28,100	KNSTD	3,750,000	240,000	KNSTD	14,415	1312	8189	887
KL15U-6X	36	94	4340	std	2	2.65	1	0	583,000	30,200	KNSTD	3,000,000	357,000	KNSTD	7768	787	6546	968
KL15U-7X	36	94	4340	std	2	2.65	1	0	553,000	19,686	KNSTD	3,120,000	277,929	KNSTD	7368	693	6809	850
Terrace T4																		
KL16D-6	36	94	4340	std	2	2.65	1	0	706,000	44,700	KNSTD	4,310,000	40,900	KNSTD	9411	1014	9418	827
KL16U-1	36	94	4340	std	2	2.65	1	0	782,167	44,495	KNSTD	4,120,000	439,000	KNSTD	10,429	1086	9001	1243
KL16U-2	36	94	4340	std	2	2.65	1	0	1,230,903	28,855	LLNL10000	6,833,708	241,474	KNSTD	16,437	1485	14,973	1414
KL16U-3	36	94	4340	std	2	2.65	1	0	1,150,000	29,000	KNSTD	5,010,000	409,000	KNSTD	15,353	1394	10,956	1313
KL16U-5	36	94	4340	std	2	2.65	1	0	790,132	31,579	LLNL10000	3,590,000	272,000	KNSTD	10,536	1010	7838	907
KL16U-6	36	94	4340	std	2	2.65	1	0	652,000	19,800	KNSTD	2,446,417	315,153	KNSTD	8690	801	5335	831
Terrace T5																		
KL17D-2	36	94	4340	std	2	2.65	1	0	840,713	39,710	LLNL10000	4,554,774	355,602	KNSTD	11,212	1112	9955	1168
KL17D-4	36	94	4340	std	2	2.65	1	0	1,195,322	44,217	KNSTD	7,820,000	930,000	KNSTD	15,960	1513	17,152	2547
KL17D-7	36	94	4340	std	2	2.65	1	0	1,271,110	60,583	LLNL10000	6,320,000	395,000	KNSTD	16,976	1689	13,840	1491
KL17U-1	36	94	4340	std	2	2.65	1	0	1,440,000	39,197	LLNL10000	6,360,000	302,000	KNSTD	19,243	1760	13,928	1388
KL17U-7	36	94	4340	std	2	2.65	1	0	2,289,167	73,908	LLNL10000	12,068,417	454,383	KNSTD	30,678	2865	26,594	2551

[a]Ages revised using the CRONUS on-line calculator V 2.2 (September 8, 2011).

[b]Code specifying how the CRONUS age calculator should treat the elevation value.

[c]Reported age is constant production rate model following scaling scheme of Lal (1991) and Stone (2000).

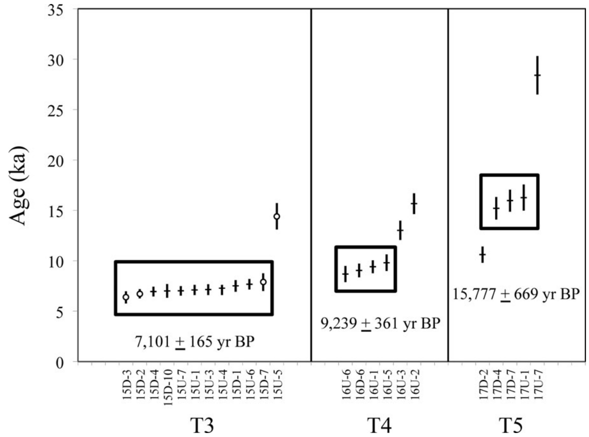

Figure 7 Cosmogenic surface exposure ages from Xidatan 2. Clast ages are averages of ^{10}Be and ^{26}Al results (cross bar), or ^{10}Be results alone (white circle). Terrace ages are weighted averages of clast dates shown inside boxes (outliers excluded). See text for details.

loess deposition on T5 at 13.9 ka (Chen et al., 2011), the 125 cm of deposits from the contact with T5 gravels to the hearth accumulated over 7496 years. This implied rate of loess deposition is 16.68 cm per 1000 years, slightly lower than typical deposition rates for the Chinese Loess Plateau (Kohfeld & Harrison, 2003: Table IV). At the inferred deposition rate, the remaining 16 cm of loess on T5 to the surface accumulated over 959 years, implying a termination of loess deposition at Xidatan around 5445 yr B.P. Archaeological materials on the T4 terrace buried at a depth of approximately 30 cm below the modern surface and 10 cm above the T4 terrace gravels. Working backwards from the inferred surface age of 5445 yr B.P., the *in situ* archaeological materials date to 7244 yr B.P. and loess deposition was initiated on T4 at around 7843 yr B.P. Given the uncertainties involved, we propose a conservative age range for the occupation of 9200–6400 yr B.P., with a peak in activities at around 7200 yr B.P.

DISCUSSION

Behavior and Biogeography

The inferred Holocene age of the Xidatan 2 occupation, between approximately 9200 and 6400 yr B.P., is younger than expected given the late Upper Paleolithic character of the assemblage (Elston et al., 1997; Brantingham, Olsen, & Schaller, 2001). The formal microblade technology seen at Xidatan 2 is a dominant feature of lithic assemblages during the terminal Pleistocene approximately 12–18 ka in northeast Asia and is commonly associated with intensification of hunting and gathering strategies in newly emerged postglacial environments (Elston et al., 1997; Brantingham et al., 2003; Elston & Brantingham, 2002). Such technologies continue to comprise a small proportion of Neolithic toolkits in North China and the Tibetan Plateau (CPAM, 1985; Lie, 1998, 1999). The bipolar technology seen at Xidatan 2, by contrast, is characteristic of the LGM in North China approximately 25–15 ka (Madsen et al., 2001; Barton, Brantingham, & Ji, 2007), and it is possible that it represents a shift toward lithic technological expediency (Nelson, 1991) under extreme climatic and environmental conditions. However, bipolar lithic technologies are alone not chronologically diagnostic. The prepared

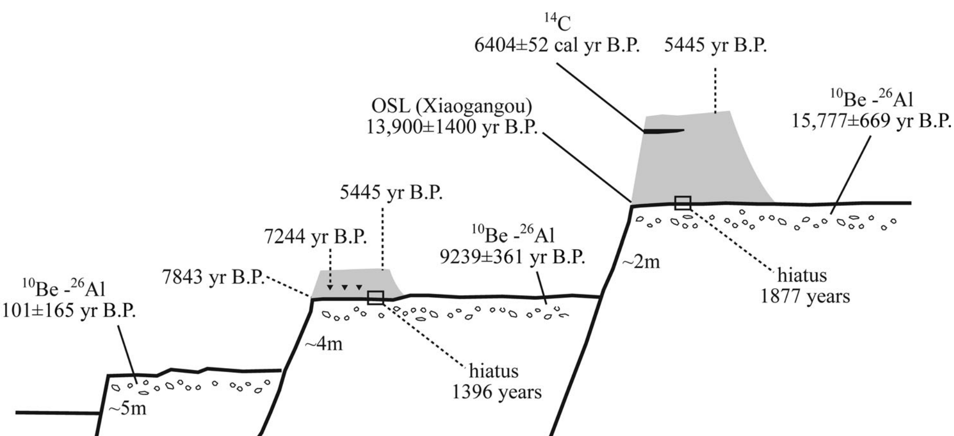

Figure 8 Sectional view of the three terraces at Xidatan 2 and the associated chronometric dates (solid lines) and inferred ages (dashed lines). The archaeological site (inverted triangles) is located on T4 and is constrained to date between approximately 9200 and 6400 yr B.P., with a peak of occupation at approximately 7244 yr B.P. ^{10}Be-^{26}Al and ^{14}C ages are from Xidatan 2. The reported OSL age on loess is from the Xiaogangou section and is taken as the earliest possible date of loess deposition in the region. Loess cap is shown in gray.

discoid core technology at Xidatan 2, like the specialized large blade and bladelet technologies of the Chang Tang (Brantingham, Olsen, & Schaller, 2001), is unknown from low-elevation contexts surrounding the Plateau. There is therefore no independent expectation for when these technologies may have first appeared. Simple core and flake tools, which are also present at Xidatan and in the Chang Tang, do not provide reliable chronological information. For example, the site of Xiao Qaidam, located north of Xidatan 2 in the Qaidam Basin at an elevation of 3100 m asl, was originally considered to be an Upper Paleolithic site dating to approximately 30 ka based on the surface collection of large quartzite cores, flakes, side scrapers, and notches and borers (Huang, Chen, & Yuan, 1987; Huang, 1994). However, we revisited the site and discovered microblade cores on that same surface, suggesting the site contains a mix of technologies similar to those found at Xidatan 2 and likely dating to a much later time period.

Overall, given the young age of Xidatan 2, but the late Upper Paleolithic character of the lithic assemblage, we favor designating the occupation as "epi-Paleolithic." We also now extend this classification to other surface archaeological assemblages recognized in the Kekexili and Chang Tang areas, south of Xidatan 2 toward the interior of the high Plateau. These sites preserve the same formal microblade technology seen at Xidatan 2 made on a similarly diverse range of raw material types. In the Kekexili area, for example, the Police Station 1 and 2 localities are dominated by microblade cores, microblades, and small-retouched tools (Figure 9). Police Station 2 also preserves examples of the prepared discoid core technology seen at Xidatan 2. Both assemblages are based on a diverse range of stone raw materials of at least five different types. The Erdaogou locality (N34.63°, E92.82°, 4765 m asl), 120 km to the southwest of Police Station 1 and 2, yielded a bullet-shaped microblade core made on obsidian as well as a large flake component. The Chang Tang assemblages, which now number more than 20, are also characterized by a prominent microblade component and a diverse array of stone raw materials, including obsidian (An, 1982; Huang, 1994; Brantingham, Olsen, & Schaller, 2001; Yuan, Huang, & Zhang, 2007). The Chang Tang site of Tsatsang contains an example of the prepared bifacial discoid core technology seen at Xidatan 2 and the Police Station 2 locality (Figure 10). These Chang Tang assemblages are unique, however, in preserving a specialized large blade and bladelet technology not seen elsewhere (Brantingham, Olsen, & Schaller, 2001). The blades are extremely flat, have very straight or gradually convergent edges, and "punctiform" striking platforms characteristic of indirect percussion or pressure flaking. Several blade and bladelet

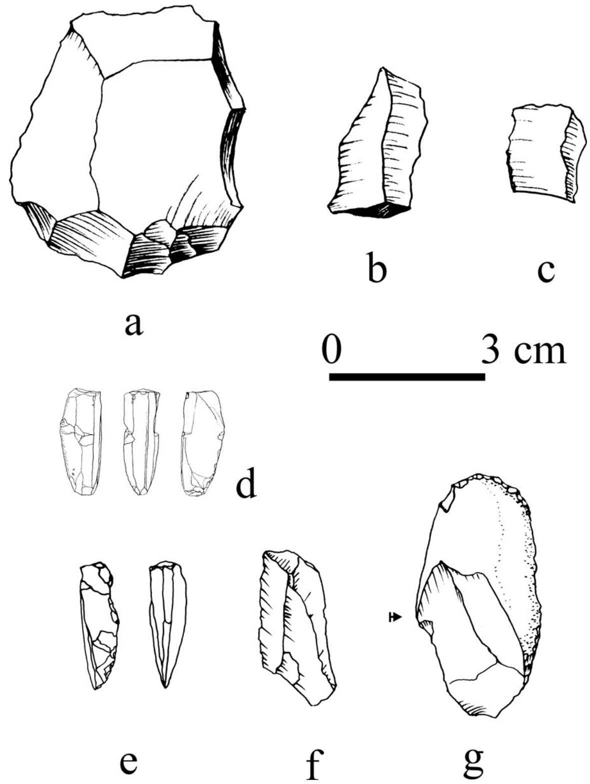

Figure 9 Lithic specimens from and the Police Station 2 (a–b) and Erdaogou (d–g) sites in the Kekexili nature reserve South of Xidatan 2. (a) flat, tablet-like flake removed from the face of a prepared discoidal cores made Police Station mudstone; (b), (c), and (f) bladelet segments; (d) and (e) "bullet-shaped" microblade cores made on obsidian and yellow jasper, respectively; (g) retouched flake scraper.

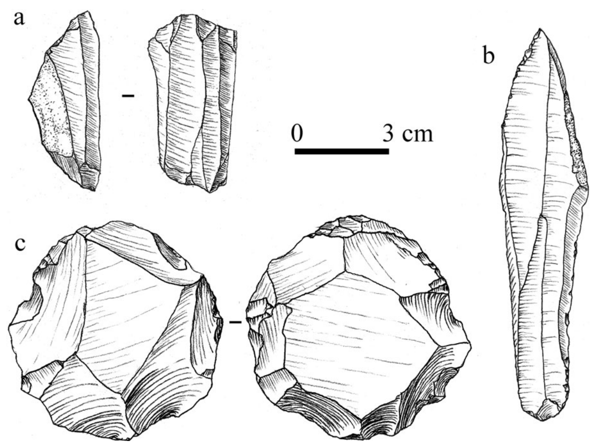

Figure 10 Lithic specimens from surface sites in the Chang Tang nature reserve. (a) bladelet core; (b) pointed prismatic blade; (c) prepared discoidal core used for producing tablet-like circular flakes.

specimens preserve lateral retouch along the margins and ventral retouch at the base, which appears to represent an accommodation for end hafting of the blades possibly as spear points (Brantingham, Olsen, & Schaller, 2001). Importantly, these blades are technologically different from the Levallois-like flat-faced blade technology seen at Shuidonggou and other northeast Asian early Upper Paleolithic sites. The uniqueness of this technology led Brantingham et al. (2001) to speculate that they were LGM in age. We now believe, however, that this large blade and bladelet technology (like the prepared discoid core technology) is derived from microblade core reduction strategies. Indeed, in many respects, the large blades of the Chang Tang are simply "scaled-up" microblades. The primary technological difference is in how they were subsequently modified for hafting and use. Similarly, the circular flakes removed from the discoidal prepared cores seen at Xidatan 2, the Police Station 2 locality and Tsatsang reflect a core reduction procedure virtually identical to that used when rejuvenating microblade core platforms. The primary technological difference here is that the resulting tablet-like flakes were derived from a flake core substrate, rather than a microblade core. Given the striking technological similarity of the Chang Tang and Kekexili materials to Xidatan 2, as well as the presence of the same obsidian at these sites, we now conclude that the Chang Tang and Kekexili assemblages are all likely early Holocene in age, contemporaneous with Xidatan 2.

The site of Xiadawu in the Maqu (Yellow River) segment of the Kunlun range, approximately 450 km east of Xidatan 2 (Van Der Woerd et al., 2002), also contains bladelet and microblade technologies comparable to Xidatan, Kekexili, and Chang Tang materials. The radiocarbon age of 11,010 cal. yr B.P. reported by Van der Woerd et al. (but ~11,300 cal. yr B.P. using more recent calibration programs) suggests that Xiadawu may be the oldest site preserving evidence of human presence on the Plateau at or above 4000 m asl. However, further work will be required to tie Xiadawu into the regional archaeological sequence. For example, the small sample from Xiadawu presently lacks the large blade component seen in the Chang Tang, and also lacks specimens of obsidian that could link the site to the central high Plateau.

In sum, we now believe that occupation of the high-elevation step of the interior Tibetan Plateau, above 4000 m asl, was *at best* extremely limited prior to the early Holocene approximately 11,000–8200 yr B.P. This conclusion differs substantially from earlier hypotheses that foragers may have moved onto the high-elevation step of the Plateau as early 25–30 ka (Brantingham et al., 2003). Recent genetically based estimates of the timing for the initial peopling of the Tibetan Plateau range from before the LGM (Zhao et al., 2009) to about 2750 yr B.P. (Yi et al., 2010) and are very inconsistent. Moreover, they are of little use in evaluating archaeologically based chronological estimates due to an uncertainty surrounding mutation rates and because many studies of the timing of adaptive mutations to high altitudes are themselves based on archaeological estimates. Sites such as Chusang and Seling Co, at elevations of 4200 and 4530 m asl, respectively, have been discussed as possible pre-Holocene occupations of the southern Tibetan Plateau (see Aldenderfer, 2007; Yuan, Huang, & Zhang, 2007; Aldenderfer, 2011). However, substantial questions surround the formation processes and dating of both of these sites.

The early Holocene age of Xidatan 2, which we also now attribute to sites in the Kekexili and Chang Tang, raises interesting questions about what processes may have driven populations, presumably dedicated foragers, to occupy the high Plateau at this time and what may have prevented them from doing so at an earlier time (Brantingham & Gao, 2006; Brantingham, Gao, Olsen et al., 2007). Holocene climatic conditions in northwest China may have favored movement of epi-Paleolithic foraging populations into higher elevation areas. The majority of paleoenvironmental proxy records from the northeastern Tibetan Plateau and its margins suggest an early Holocene period of increased effective moisture (see Herzschuh et al., 2006; Mügler et al., 2010), but an increasing number of records from the region indicate this period of optimal climatic conditions occurred somewhat later, during the Mid-Holocene (e.g., Zhao, Yu, & Zhao, 2011). The differences are a matter of a few thousand years, however, and regardless of the eventual resolution, conditions on the Tibetan Plateau were wetter and warmer during the early-to-middle Holocene than during the LGM and the Pleistocene/Holocene transition. A local record of eolian deposition downstream from Xidatan in the eastern Qaidam basin suggests conditions were arid from approximately 12.4 to 11.5 ka (and probably during the Younger Dryas) and increasingly humid approximately 10 to 8 ka. Maximum Holocene effective moisture occurred approximately 8–4.5 ka, with a return to relatively arid conditions after approximately 4.5 ka (Yu & Lai, 2012). If confirmed, this suggests the occupation of Xidatan occurred during a period of increasing to maximum effective moisture that may have caused faunal populations to flourish and may have "pulled" epi-Paleolithic foragers onto the high Plateau.

It is also possible that epi-Paleolithic foragers were driven to occupy more extreme habitats after 9.2 ka by expanding agricultural populations in low-elevation environments (Brantingham & Gao, 2006; Brantingham, Gao, Olsen et al., 2007; see also Spielmann & Eder, 1994). An, Feng, and Tang (2004) argue that warm-wet conditions on the Western Loess Plateau encouraged the emergence and subsequent florescence of Neolithic Dadiwan (~7800–7350 yr B.P.) and early Yangshao (6800–6000 yr B.P.) cultures (see also Lie, 1999; An et al., 2005). With fewer foraging options in prime low-elevation habitats, foragers may have been pushed to higher elevations on a more permanent basis through a process of competitive exclusion (Brantingham & Gao, 2006; Brantingham, Gao, Olsen et al., 2007).

It is still an open question, however, why foragers may not have moved onto the high Plateau at earlier times. There is some evidence that early and late Upper Paleolithic foragers were exploiting parts of the Qaidam basin, between approximately 3000 and 4000 m asl, during the late Pleistocene (Brantingham & Gao, 2006; Madsen et al., 2006; Brantingham, Gao, Olsen et al., 2007). These occupations appear to represent only seasonal exploitation of lake basins with easy access to low-elevation habitats. For example, a number of stratified sites on the southern shore of Qinghai Lake, dated between approximately 15,000 and 12,000 yr B.P., represent short-term encampments where small foraging groups engaged in intensive processing of medium and small game (Madsen et al., 2006).

While it is difficult to determine the season of occupation at these sites, there is no evidence to suggest that they were long-term habitation sites, and their proximity to major mountain passes leading to low-elevation habitats suggests that they could have been exploited easily as part of specialized seasonal movements to higher elevations (Zeanah, 2004). While a few of these seasonal foragers may have reached the margins of the high Plateau, the absence of substantial populations on the interior at this time may reflect a general deficiency in early and late Upper Paleolithic adaptations to ensure survival at such environmental extremes. In this case, the specialized large blade and bladelet technologies seen in the Chang Tang during the early Holocene may reflect part of an adaptive shift needed to allow more complete exploitation of the high Plateau at this time. However, the current absence of evidence for high Plateau occupations during the early and late Upper Paleolithic also may simply reflect the absence of pressures that would have created incentive to move to high-elevation extremes. Therefore, we cannot rule out the possibility that early and late Upper Paleolithic adaptations were in fact sufficient to ensure survival at high elevation (Brantingham & Gao, 2006; Brantingham, Gao, Olsen et al., 2007).

It is similarly difficult to argue conclusively that the early Holocene occupation at Xidatan 2 represents anything more than seasonal exploitation of a high-elevation habitat. The primary evidence in favor of a model of full-time, year-round occupation of the high Plateau at this time is the sheer size of the territory exploited. While the Pleistocene forager sites in the Qinghai Lake basin are less than 100 km from low-elevation habitats off of the Plateau (Brantingham et al., 2003; Madsen et al., 2006), Xidatan 2 and the correlated surface sites in the Kekexili and Chang Tang nature reserves are many hundreds of kilometers from any point of descent. For example, the shortest linear distance between Xidatan 2 and habitats below 2500 m asl is approximately 475 km. But whether or not mobility over such distances reflects seasonal, or year-round occupation depends in large measure upon what we assume about the organization of mobility and the associated costs of movement (Brantingham, 2003, 2006). The cumulative distance traveled by arctic foragers over an annual round of residential moves may reach 600–700 km (Kelly, 1995). Given the potentially high costs of mobility at high elevation (Aldenderfer, 1998), it may be reasonable to hypothesize that sites in the Kekexili and Chang Tang reserves, which are even farther from low-elevation habitats than Xidatan 2, represent year-round occupation. However, there is also good evidence from Eastern Europe, stretching back as far as the Middle Paleolithic, that stone raw materials were regularly transported over distances of 300–400 km and occasionally as much as 800–1000 km (Féblot-Augustins, 1997b).

It remains possible therefore that Xidatan 2 was part of a settlement system involving very long-distance moves onto and off of the high-elevation step of the Plateau. The occurrence of Chang Tang obsidian at the Qinghai Lake site of Jiangxigou 2, nearly 1000 km away along a straight line from the source of this material, demonstrates that by 8–6 ka groups of people were moving between the middle- and high-elevation steps of the Plateau, at least on occasion. Such a strategy would have mandated that most occupations would be very short in duration. In this regard, Surovell (2009) has shown that the stone raw material richness at a site may serve as a reliable proxy measure of occupation duration. In general, as site occupation span increases, the stone used at a site comes to be dominated by a single raw material type. Sites that are occupied repeatedly for short-term foraging purposes tend to contain many different nonlocal stone types. The latter is a good qualitative characterization of the situation at Xidatan 2, where at least seven distinct types and perhaps 21 varieties of stone are represented.

While it may be reasonable to conclude that Xidatan 2 represents repeated, short-term occupations by highly mobile foragers, the small lithic assemblage still provides only a limited picture of behavior at the site. The topographic setting of Xidatan 2 in a steep, glacial-cut drainage would be ideal for organizing game drives, and what ecological data exist (see Schaller, 1998) suggest that game would have been abundant on the Plateau during the time of occupation. Brantingham et al. (2001) argued elsewhere that a specialized large-blade technology seen on the high Plateau in the Chang Tang was designed to supply end-hafted spear points, a specialization not seen in lower elevation contexts. While examples of end-hafted blades have not been found at Xidatan 2, the prominence of microblades and microblade cores may imply the use of modular inset points as a key piece of hunting gear (Elston & Brantingham, 2002). However, the absence of faunal remains from the Xidatan 2 site means that we are unable to either confirm or reject the hypothesis that the Xidatan 2 occupation was tied to a large-game subsistence focus and that such a strategy was necessary to support occupation of the high Plateau.

Ultimately, additional evidence must be brought to bear on the problem of when full-time, year-round occupation of the Tibetan Plateau was finally established and what behavioral strategies made full-time occupation possible. If such occupations were possible through a strict foraging adaptation, then one would expect to see sites with zooarchaeological remains in abundances commensurate with the need for long-term supply (especially at winter camps) and probably also more substantial architectural and food storage features. Based on these criteria, the only unequivocal evidence for year-round occupation of the Tibetan Plateau above 3000 m postdates 6000 yr B.P. and is associated with the radiation of agricultural groups out of low-elevation areas (Brantingham & Gao, 2006; Brantingham, Gao, Olsen et al., 2007). The site of Karuo, near the modern town of Qamdo at approximately 3100 and 3200 m asl, represents this radiation (CPAM, 1985; Aldenderfer & Zhang, 2004).

CONCLUSIONS

Xidatan 2, located in the Kunlun Pass area of Qinghai Province at an elevation of 4300 m asl, provides evidence of human occupation of the high-elevation Tibetan Plateau during the early Holocene. ^{10}Be-^{26}Al cosmogenic surface exposure ages, combined with OSL and AMS radiocarbon ages, indicate that the site was occupied between approximately 9200 and 6400 yr B.P. Archaeological materials recovered from associated surface and buried contexts at Xidatan 2 include specialized microblade technologies characteristic of the northeast Asian late Upper Paleolithic and epi-Paleolithic as well as discoidal prepared core and bipolar flake technologies. These materials document use of the site by high mobility foraging groups, who may have engaged in seasonal foraging rounds that carried them onto and off of the high-elevation Plateau. Raw materials present at the site, including a true obsidian, are traced to other archaeological occurrences on the high Plateau, south of the Kunlun Pass, and to an early Holocene archaeological site in the Qinghai Lake basin. This evidence demonstrates that stone transport occurred regularly over distances of approximately 500 km, and occasionally over distances as great as approximately 1000 km, and that movement between the high- and middle-elevation steps of the Plateau was a feature of settlement systems by approximately 8000 yr B.P.

This research was supported in part by the U.S. National Science Foundation (SBE 0214870 and 0841435) and the Chinese National Science Foundation. We thank three anonymous reviewers for the helpful comments.

REFERENCES

Aldenderfer, M. (2011). Peopling the Tibetan Plateau: Insights from Archaeology. High Altitude Medicine & Biology, 12(2), 141–147.

Aldenderfer, M., & Zhang, Y.N. (2004). The prehistory of the Tibetan plateau to the seventh century AD: Perspectives and research from China and the West since 1950. Journal of World Prehistory, 18(1), 1–55.

Aldenderfer, M.S. (1998). Montane foragers: Asana and the south-central Andean Archaic. Iowa City, IA: University of Iowa Press.

Aldenderfer, M.S. (2003). Moving up in the world. American Scientist, 91(6), 542–549.

Aldenderfer, M.S. (2007). Modeling the Neolithic on the Tibetan Plateau. In D.B. Madsen, F.H. Chen, & X. Gao (Eds.), Human adaptation to climate change in arid China (pp. 151–165). Amsterdam: Elsevier.

An, C.B., Feng, Z.D., & Tang, L.Y. (2004). Environmental change and cultural response between 8000 and 4000 cal. yr BP in the western Loess Plateau, northwest China. Journal of Quaternary Science, 19(6), 529–535.

An, C.B., Tang, L.Y., Barton, L., & Chen, F.H. (2005). Climate change and cultural response around 4000 cal yr BP in the western part of Chinese Loess Plateau. Quaternary Research, 63(3), 347–352.

An, Z. (1982). Paleoliths and microliths from Shenjia and Shuanghu, northern Tibet. Current Anthropology, 23, 493–499.

Balco, G., Stone, J.O., Lifton, N.A., & Dunai, T.J. (2008). A complete and easily accessible means of calculating surface exposure ages or erosion rates from 10Be and 26Al measurements. Quaternary Geochronology, 3(3), 174–195.

Barton, L., Brantingham, P.J., & Ji, D. (2007). Late Pleistocene climate change and Paleolithic cultural evolution in Northern China: Implications from the Last Glacial Maximum. In D.B. Madsen, F.H. Chen, & X. Gao (Eds.), Human adaptation to climate change in Arid China (pp. 105–128). Amsterdam: Elsevier.

Benn, D.I., & Owen, L.A. (1998). The role of the Indian summer monsoon and the mid-latitude westerlies in Himalayan glaciation: Review and speculative discussion. Journal of the Geological Society of London, 155, 353–363.

Brantingham, P.J. (2003). A neutral model of stone raw material procurement. American Antiquity, 68(3), 487–509.

Brantingham, P.J. (2006). Measuring forager mobility. Current Anthropology, 47, 435–459.

Brantingham, P.J., & Gao, X. (2006). Peopling of the northern Tibetan Plateau. World Archaeology, 38, 387–414.

Brantingham, P.J., Olsen, J.W., Rech, J.A., & Krivoshapkin, A.I. (2000). Raw material quality and prepared core technologies in Northeast Asia. Journal of Archaeological Science, 27, 255–271.

Brantingham, P.J., Krivoshapkin, A.I., Li, J., & Tserendagva, Y. (2001). The initial Upper Paleolithic in Northeast Asia. Current Anthropology, 42, 735–746.

Brantingham, P.J., Olsen, J.W., & Schaller, G.B. (2001). Lithic assemblages from the Chang Tang Region, northern Tibet. Antiquity, 75, 319–327.

Brantingham, P.J., Haizhou, M.A., Olsen, J.W., Gao, X., Madsen, D.B., & Rhode, D.E. (2003). Speculation on the timing and nature of Late Pleistocene hunter-gatherer colonization of the Tibetan Plateau. Chinese Science Bulletin, 48(14), 1510–1516.

Brantingham, P.J., Li, J., Madsen, D.B., Gao, X., Bettinger, R.L., & Elston, R.G. (2004). The initial Upper Paleolithic at Shuidonggou, Northwest China. In P.J. Brantingham, S.L. Kuhn, & K.W. Kerry (Eds.), The early Upper Paleolithic beyond Western Europe. Berkeley: University of California Press.

Brantingham, P.J., Gao, X., Olsen, J.W., Ma, H., Rhode, D., Zhang, H., & Madsen, D.B. (2007). A short chronology for the peopling of the Tibetan Plateau. In D.B. Madsen, F.H. Chen, & X. Gao (Eds.), Human adaptation to climate change in arid China (pp. 129–150). Amsterdam: Elsevier.

Chen, Y., Li, Y., Zhang, Y., Zhang, M., Zhang, J., Yi, C., & Liu, G. (2011). Late quaternary deposition and incision sequences of the Golmud River and their environmental implications. Quaternary International, 236(1–2), 48–56.

CPAM. (1985). Karou: A Neolithic site in Tibet. Beijing: Cultural Relics Publishing House.

Elston, R.G., & Brantingham, P.J. (2002). Microlithic technology in Northeast Asia: A risk minimizing strategy of the late Paleolithic and early Holocene. In R.G. Elston & S.L. Kuhn (Eds.), Thinking small: Global perspectives on microlithization (pp. 103–116). Archaeological Papers of the American Anthropological Association, 12(1).

Elston, R.G., Xu, C., Madsen, D.B., Zhong, K., Bettinger, R.L., Li, J., Brantingham, P.J., Wang, H., & Yu, J. (1997). New dates for the Chinese Mesolithic. Antiquity, 71, 985–993.

Faure, G., & Mensing, T.M. (2005). Isotopes: Principles and applications. Hoboken, NJ: John Wiley and Sons.

Féblot-Augustins, J. (1997b). La Circulation des Matières Premières au Paléolithique: Synthèse des Données Perspectives Comportementales, Vol. 1. Liège: Université de Liège.

Fielding, E., Isacks, B., Barazangi, M., & Duncan, C. (1994). How flat is Tibet? Geology, 22(2), 163–167.

Gao, X. (2000). A study of flaking technology at Zhoukoudian Locality 15. Acta Anthropologica Sinica, 19, 199–215.

Gao, X., Pei, S., Wang, H., & Zhong, K. (2004). A report on Paleolithic reconnaissance in Ningxia, North China. Acta Anthropologica Sinica, 23, 307–325.

Gosse, J.C., & Phillips, F.M. (2001). Terrestrial in situ cosmogenic nuclides: Theory and application. Quaternary Science Reviews, 1475–1560.

Harris, S.A., Cui, Z.J., & Cheng, G.D. (1998). Origin of a bouldery diamicton, Kunlun pass, Qinghai-Xizang plateau, People's Republic of China: Gelifluction deposit or rock glacier? Earth Surface Processes And Landforms, 23(10), 943–952.

Herzschuh, U., Winter, K., Wunnemann, B., & Li, S.J. (2006). A general cooling trend on the central Tibetan Plateau throughout the Holocene recorded by the Lake Zigetang pollen spectra. Quaternary International, 154, 113–121.

Huang, W. (1994). The prehistoric human occupation of the Qinghai-Xizang Plateau. Gottinger Geographische Abhandlungen, 95, 201–219.

Huang, W., Chen, K., & Yuan, B. (1987). Discovery of Paleolithic artifacts in the Xiao Qaidam Lake area, Qinghai Province. Beijing: Sciences Press.

Ji, D., Chen, F., Bettinger, R.L., Elston, R.C., Geng, Z., Barton, L.W., Wang, H., An, C., & Zhang, D. (2005). Human response to the Last Glacial Maximum: Evidence from North China. Acta Anthropologica Sinica, 24, 270–282.

Jin, Z.D., Wu, Y.H., Zhang, X.H., & Wang, S.M. (2005). Role of late glacial to mid-Holocene climate in catchment weathering in the central Tibetan Plateau. Quaternary Research, 63(2), 161–170.

Kelly, R.L. (1995). The foraging spectrum: Diversity in hunter-gatherer lifeways. Washington, D.C.: Smithsonian Institution Press.

Kohfeld, K.E., & Harrison, S.P. (2003). Glacial-interglacial changes in dust deposition on the Chinese loess plateau. Quaternary Science Reviews, 22(18–19), 1859–1878.

Kuhn, S.L. (1995). Mousterian lithic technology: An ecological perspective. Princeton, NJ: Princeton University Press.

Küster, Y., Hetzel, R., Krbetschek, M., & Tao, M. (2006). Holocene loess sedimentation along the Qilian Shan (China): Significance for understanding the processes and timing of loess deposition. Quaternary Science Reviews, 25(1–2), 114–125.

Lal, D. (1991). Cosmic-ray labeling of erosion surfaces—In situ nuclide production-rates and erosion models. Earth and Planetary Science Letters, 104(2–4), 424–439.

Lehmkuhl, F., & Haselein, F. (2000). Quaternary paleoenvironmental change on the Tibetan Plateau and adjacent areas (western China and western Mongolia). Quaternary International, 65–6, 121–145.

Li, C.G., Yin, H.F., & Yu, Q.W. (2000). Evolution of drainage systems and its developing trend in connection with tectonic uplift of Eastern Kunlun Mt. Chinese Science Bulletin, 45(20), 1904–1908.

Lie, D. (1998). The microblade tradition in China: Regional chronologies and significance in the transition to Neolithic. Asian Perspectives, 37, 84–112.

Lie, D. (1999). The transition from foraging to farming and the origin of agriculture in China. Oxford: British Archaeological Reports International Series 774.

Lu, H., Zhao, C., Mason, J., Yi, S., Zhao, H., Zhou, Y., Ji, J., Swinehart, J., & Wang, C. (2011). Holocene climatic changes revealed by aeolian deposits from the Qinghai Lake area (northeastern Qinghai-Tibetan Plateau) and possible forcing mechanisms. Holocene, 21(2), 297–304.

Madsen, D.B., Li, J., Elston, R.G., Xu, C., Bettinger, R.L., Brantingham, P.J., & Zhong, K. (1998). The loess/paleosol record and the nature of the younger dryas climate in central China. Geoarchaeology, 13, 847–869.

Madsen, D.B., Li, J., Brantingham, P.J., Gao, X., Elston, R.G., & Bettinger, R.L. (2001). Dating Shuidonggou and the upper Paleolithic blade industry in North China. Antiquity, 75, 706–716.

Madsen, D.B., Ma, H., Brantingham, P.J., Gao, X., Rhode, D., Zhang, H., & Olsen, J. (2006). The late Upper Paleolithic occupation of the northern Tibetan Plateau margin. Journal of Archaeological Science, 33, 1433–1444.

Madsen, D.B., Ma, H.Z., Rhode, D., Brantingham, P.J., & Forman, S.L. (2008). Age constraints on the late quaternary evolution of Qinghai Lake, Tibetan Plateau. Quaternary Research, 69(2), 316–325.

Morrill, C., Overpeck, J.T., & Cole, J.E. (2003). A synthesis of abrupt changes in the Asian summer monsoon since the last deglaciation. Holocene, 13(4), 465–476.

Mügler, I., Gleixner, G., Günther, F., Mäusbacher, R., Daut, G., Schütt, B., Berking, J., Schwalb, A., Schwark, L., Xu, B., Tao, Y., Zhu, L., & Yi, C. (2010). A multi-proxy approach to reconstruct hydrological changes and Holocene climate development of Nam Co, Central Tibet. Journal of Paleolimnology, 43(4), 625–648.

Nelson, M.C. (1991). The study of technological organization. Archaeological Method and Theory, 3, 57–100.

Nishiizumi, K., Imamura, M., Caffee, M.W., Southon, J.R., Finkel, R.C., & McAninch, J. (2007). Absolute calibration of 10Be AMS standards. Nuclear Instruments and Methods in Physics Research Section B: Beam Interactions with Materials and Atoms, 258(2), 403–413.

Owen, L.A., Finkel, R.C., Ma, H., & Barnard, P.L. (2006). Late Quaternary landscape evolution in the Kunlun Mountains and Qaidam Basin, northern Tibet: A framework for examining the links between glaciation, lake level changes and alluvial fan formation. Quaternary International, 154–155, 73–86.

Rhode, D., Zhang, H.Y., Madsen, D.B., Xing, G., Brantingham, R.J., Ma, H.Z., & Olsen, J.W. (2007). Epipaleolithic/early Neolithic settlements at Qinghai Lake, western China. Journal of Archaeological Science, 34(4), 600–612.

Rhode, D., Haizhou, M., Madsen, D., Brantingham, P., Forman, S., & Olsen, J. (2009). Paleoenvironmental and archaeological investigations at Qinghai Lake, western China: Geomorphic and chronometric evidence of lake level history. Quaternary International, 218(1–2), 29–44.

Ryerson, F.J., Tapponnier, P., Gaudemer, Y., Finkel, R., Meriaux, A.S., Caffee, M., Zhao, G., & He, Q. (1998). Holocene left-slip rate determined by cosmogenic surface dating on the Xidatan segment of the Kunlun fault (Qinghai, China). Geology, 26(8), 695–698.

Schaller, G.B. (1998). Wildlife of the Tibetan steppe. Chicago, IL: University of Chicago Press.

Spielmann, K.A., & Eder, J.F. (1994). Hunters and farmers—then and now. Annual Review of Anthropology, 23, 303–323.

Stone, J.O. (2000). Air pressure and cosmogenic isotope production. Journal Of Geophysical Research-Solid Earth, 105(B10), 23753–23759.

Sun, J., Li, S.-H., Muhs, D.R., & Li, B. (2007). Loess sedimentation in Tibet: Provenance, processes, and link with quaternary glaciations. Quaternary Science Reviews, 26(17–18), 2265–2280.

Surovell, T.A. (2009). Toward a behavioral ecology lithic technology: Cases from Paleoindian archaeology. Tucson, AZ: University of Arizona Press.

Tapponnier, P., & Molnar, P. (1977). Active faulting and tectonics in China. Journal of Geophysical Research, 82(20), 2905–2930.

Tapponnier, P., Xu, Z.Q., Roger, F., Meyer, B., Arnaud, N., Wittlinger, G., & Yang, J. (2001). Geology—Oblique stepwise rise and growth of the Tibet plateau. Science, 294(5547), 1671–1677.

Van Der Woerd, J., Tapponnier, P., Ryerson, F.J., Meriaux, A.S., Meyer, B., Gaudemer, Y., Finkel, R., Caffee, M., Zhao, G., & Xu, Z. (2002). Uniform postglacial slip-rate along the central 600 km of the Kunlun Fault (Tibet), from Al-26, Be-10, and C-14 dating of riser offsets, and climatic origin of the regional morphology. Geophysical Journal International, 148(3), 356–388.

Van Der Woerd, J., Owen, L.A., Tapponnier, P., Xu, X.W., Kervyn, F., Finkel, R.C., & Barnard, P. (2004). Giant, similar to M8 earthquake-triggered ice avalanches in the eastern Kunlun Shan, northern Tibet: Characteristics, nature and dynamics. Geological Society Of America Bulletin, 116(3–4), 394–406.

Wang, A., Wang, G., & Xiang, S. (2003). Characteristics of river terraces in north slope of eastern Kunlun Mountains and their relationship with plateau uplift. Earth Science—Journal of China University of Geosciences, 28(6), 675–679.

Wang, A., Smith, J.A., Wang, G., Zhang, K., Xiang, S., & Liu, D. (2009). Late quaternary river terrace sequences in the eastern Kunlun Range, northern Tibet: A combined record of climatic change and surface uplift. Journal of Asian Earth Sciences, 34(4), 532–543.

Wu, T.H., Li, S.X., Cheng, G.D., & Nan, Z.T. (2005). Using ground-penetrating radar to detect permafrost degradation in the northern limit of permafrost on the Tibetan Plateau. Cold Regions Science And Technology, 41(3), 211–219.

Wu, Y.Q., Cui, Z.J., Liu, G.N., Ge, D.K., Yin, J.R., Xu, Q.H., & Pang, Q. (2001). Quaternary geomorphological evolution of the Kunlun Pass area and uplift of the Qinghai-Xizang (Tibet) Plateau. Geomorphology, 36(3–4), 203–216.

Yang, B., Shi, Y.F., Braeuning, A., & Wang, J.X. (2004). Evidence for a warm-humid climate in arid northwestern China during 40–30ka BP. Quaternary Science Reviews, 23(23–24), 2537–2548.

Yi, X., Liang, Y., Huerta-Sanchez, E., Jin, X., Cuo, Z.X.P., Pool, J.E., Xu, X., Jiang, H., Vinckenbosch, N., Korneliussen, T.S., Zheng, H., Liu, T., He, W., Li, K., Luo, R., Nie, X., Wu, H., Zhao, M., Cao, H., Zou, J., Shan, Y., Li, S., Yang, Q., Asan, Ni, P., Tian, G., Xu, J., Liu, X., Jiang, T., Wu, R., Zhou, G., Tang, M., Qin, J., Wang, T., Feng, S., Li, G., Huasang, Luosang, J., Wang, W., Chen, F., Wang, Y., Zheng, X., Li, Z., Bianba, Z., Yang, G., Wang, X., Tang, S., Gao, G., Chen, Y., Luo, Z., Gusang, L., Cao, Z., Zhang, Q., Ouyang, W., Ren, X., Liang, H., Zheng, H., Huang, Y., Li, J., Bolund, L., Kristiansen, K., Li, Y., Zhang, Y., Zhang, X., Li, R., Li, S., Yang, H., Nielsen, R., Wang, J., & Wang, J. 2010. Sequencing of 50 human exomes reveals adaptation to high altitude. Science. 329(5987):75–78. doi: 10.1126/science.1190371.

Yin, A., & Harrison, T.M. (2000). Geologic evolution of the Himalayan-Tibetan orogen. Annual Review Of Earth And Planetary Sciences, 28, 211–280.

Yu, L., & Lai, Z. (2012). OSL chronology and palaeoclimatic implications of aeolian sediments in the eastern Qaidam Basin of the northeastern Qinghai-Tibetan Plateau. Palaeogeography, Palaeoclimatology, Palaeoecology, 337–338(0), 120–129.

Yuan, B.Y., Huang, W.W., & Zhang, D. (2007). New evidence for human occupation of the northern Tibetan Plateau, China during the late Pleistocene. Chinese Science Bulletin, 52(19), 2675–2679.

Zeanah, D.W. (2004). Sexual division of labor and central place foraging: A model for the Carson Desert of western Nevada. Journal of Anthropological Archaeology, 23(1), 1–32.

Zhang, D.D., & Li, S.H. (2002). Optical dating of Tibetan human hand- and footprints: An implication for the palaeoenvironment of the last glaciation of the Tibetan Plateau. Geophysical Research Letters, 29(5), 16-2–16-3.

Zhang, S. (1999). A study of stone artifacts found at the Xiaokouzi Prehistoric Site. Acta Anthropologica Sinica, 18, 81–101.

Zhao, M., Kong, Q., Wang, H., Peng, M., Xie, X., Wang, W., Jiayang, Duan, J., Cai, M., Zhao, S., Cidanpingcuo, Tu, Y., Wu, S., Yao, Y., Bandelt, H.J., & Zhang, Y. (2009). Mitochondrial genome evidence reveals successful Late Paleolithic settlement on the Tibetan Plateau. Proceedings of the National Academy of Sciences, 106(50), 21230–21235.

Zhao, Y., Yu, Z., & Zhao, W. (2011). Holocene vegetation and climate histories in the eastern Tibetan Plateau: Controls by insolation-driven temperature or monsoon-derived precipitation changes? Quaternary Science Reviews, 30(9–10), 1173–1184.

